Air Qual Atmos Health (2015) 8:483–494
DOI 10.1007/s11869-014-0297-0

Temporal change of PM_{10} and its mass fraction during a dust storm in September 2009 in Australia

Rupak Aryal · Simon Beecham · Mohammad Kamruzzaman · Samantha Conner · Byeong-Kyu Lee

Received: 21 July 2014 / Accepted: 19 September 2014 / Published online: 30 September 2014

Abstract Frequent dust storms are a major concern in Australia due to associated human health risks and potential economic losses. From 23 to 24 September 2009, a dust storm passed over many east coast regions of Australia. This blanketed them with dust and reduced the visibility to a few hundred meters for several hours. The respirable particulate matter less than 10 μm (PM_{10}) was monitored at 22 locations across New South Wales (NSW) by the Environmental Protection Agency. In addition, samples were collected in Sydney using a nine-stage cascade impactor both during and after the dust storm. The PM_{10} concentration over most of NSW jumped from less than 50 μg/m^3 to more than 10,000 μg/m^3 within a couple of hours and then dropped again to more normal levels (<50 μg/m^3). The normal bimodal particle size distribution was observed to change to a multi-modal distribution during a dust storm event. Also, the elemental ratio of Al to Si increased from 0.14 to 0.39 during the storm. An Al/Si ratio >0.3 indicates that the dust originated from inland desert areas and indeed was closely matched to Lake Eyre Basin crustal element data indicating it had travelled from central Australia to the eastern coasts.

Keywords PM_{10} · Dust storm · Particle size distribution · Mineralogical content

R. Aryal (✉) · S. Beecham · M. Kamruzzaman
Centre for Water Management and Reuse, School of Natural and Built Environments, University of South Australia, Mawson Lakes 5095, SA, Australia
e-mail: rupak.aryal@unisa.edu.au

S. Conner
Bureau of Meteorology, Kent Town, SA 5067, Australia

B.-K. Lee
School of Civil Engineering, University of Ulsan, Ulsan 680-749, Korea

Introduction

Particulate matter in urban areas has become a major concern due to the risks posed to both human and ecosystem health (Ayala et al. 2012). Particulate matter in urban areas can be partly derived from wind erosion of soils, including both urban soils, as well as rural and agricultural soils transported over long distances. They can also, to a lesser extent, derive from mechanical disturbance by vehicular, commercial, and industrial activities in urban areas (Aryal et al. 2008; Lee and Lee 2008). Respirable particulate matter, which are those particulates less than 10 μm in diameter (known as PM_{10}), are particularly important as a measure of air pollution in a given area (Kuenzli et al. 2000; Lim et al. 2010; Lu 2002; Ragosta et al. 2006). Several studies have documented the relationship between particulate matter and diseases such as respiratory cardiovascular disease and lung diseases (Donaldson and MacNee 2001; Goldberg et al. 2006; Kan and Chen 2003; Mehta et al. 2013). It has also been documented that mortality rates increase by 1 % and incidents of respirable diseases increase by 3–6 % when PM_{10} is increased by only 10 μg/m^3 (Ostro et al. 1999). PM_{10} is a major concern for countries such as China, Japan, Korea, Australia, and Spain that receive frequent dust storms (Ekström et al. 2004; Kim et al. 2001; Lyamani et al. 2005; Vanderstraeten et al. 2008; Watanabe et al. 2011; Xie et al. 2005). Overall dust storms are a natural phenomena that can affect very large areas to such an extent that both local and national economies can be impacted (Stefanski and Sivakumar 2009; Tozer and Leys 2013; Wang et al. 2006).

Over the last two decades, dust storms along the Australian east coast have become a subject of interest due to their adverse impacts on human health and the economy in many major cities such as Sydney, Canberra, and Brisbane. It is reported that the Lake Eyre Basin is one of the major active dust storm regions in Australia (McTainsh et al. 1998; Middleton 1984) and the eighth most active dust source region in the world (Washington et al. 2003). The Lake Eyre Basin covers almost one sixth of the area of Australia (Strong et al. 2011). According to previous studies, dust activity is higher in the Lake Eyre Basin during late spring (September–October) and early summer (November–December) (Ekström et al. 2004). Figure 1a shows the dust storm origin of Lake Eyre Basin and the storm pathways across Australia.

On 23 September 2009, many towns and cities in the east of Australia were affected by a dust storm generated the previous afternoon in the vicinity of the Lake Eyre Basin. The passage of a vigorous trough of low pressure generated damaging winds had developed during 22 September in central South Australia (Fig. 2). Mean winds of 60–70 km/h (16–19 m/s) and gusts up to 80–90 km/h (22–25 m/s) were also recorded in centers such as Coober Pedy, Marree, and Oodnadatta.

The windy conditions combined with an unstable atmosphere lifted the dust particles into the air. The dust was then transported toward the east in winds recorded as being between 80 and 105 km/h (22–29 m/s) at heights between 1 and 1.8 km above ground level. Major cities such as Sydney and Brisbane were blanketed with dust for nearly 24 h before the storm headed to the Tasman Sea (Aryal et al. 2012). Since the dust storm travelled through the Lake Eyre Basin and agricultural land, the dust was believed to contain large amounts of desert sand as well as top soil from agricultural land. Indeed, it was reported that this particular event carried away over 75,000 t per hour of soil (Tozer 2012) while 71,015 t per hour of soil loss was also reported by Leys et al. (2011). Numerous studies have investigated the composition and have attempted to model the possible source of Australian dust storms using data on mineral loadings in the atmosphere, surface material characteristics (Aryal et al. 2012), and transport models (Knight et al. 1995; Radhi et al. 2010a, b). It has been said that the dust particles had a density that was almost 70 times higher than normal (Li et al. 2010). The PM_{10} dynamics and the particle size distribution mass fraction recorded in Brisbane during the event were compared with normal days by Jayaratne et al. (2011). Brisbane is located almost 1,000 km north of Sydney. They observed that the storm peaked at about mid-day on 22 September when the hourly average $PM_{2.5}$ and PM_{10} values reached 814 and 6,460 μg m^{-3} and added that the PM_{10} fraction accounted for about 68 % of the total mass. Leys et al. (2011) discussed mass transport of the PM_{10} in the New South Wales (NSW) region; however, they did not report either the particle size distribution within the PM_{10} or its elemental composition. This paper elaborates discussion on the transport of PM_{10} in the NSW region during an event, the particle size distribution within PM_{10} with a comparison of normal PM_{10} levels and

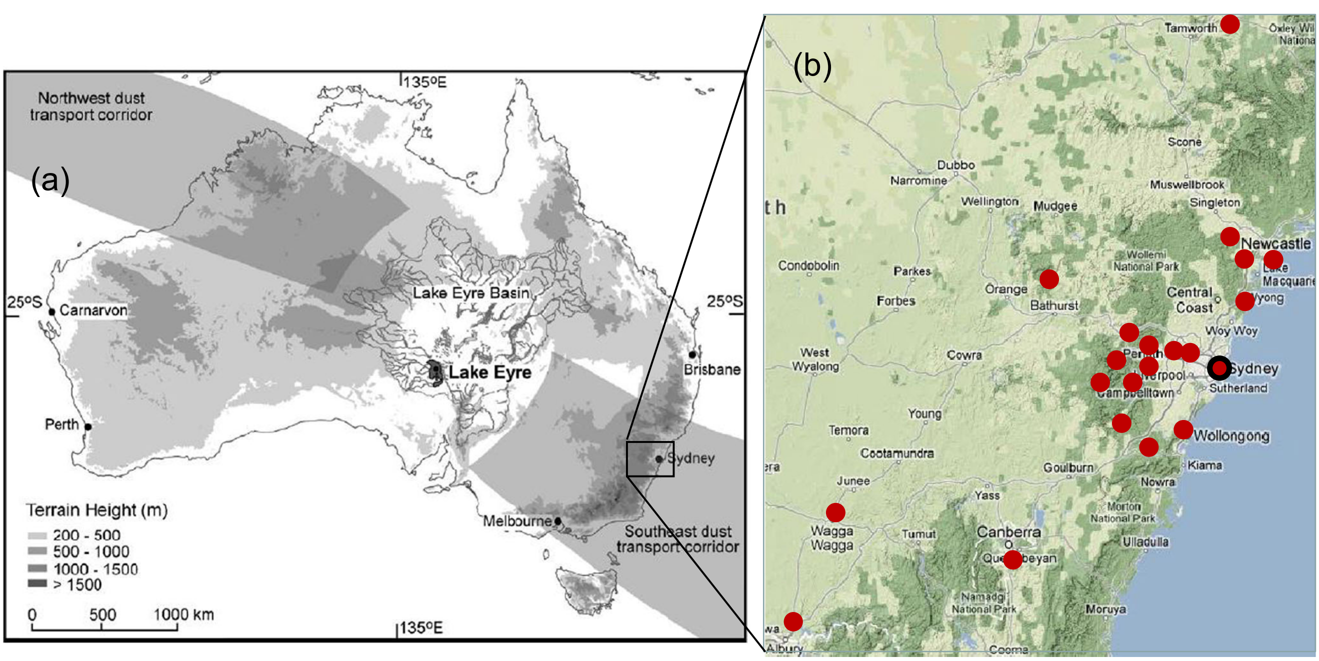

Fig. 1 **a** Location map showing Lake Eyre Basin and the dust transport corridor (*shaded*) proposed by Bowler (1976) and **b** PM_{10} sampling sites across NSW (*black circles* show the PM_{10} fraction sampling sites in Sydney)

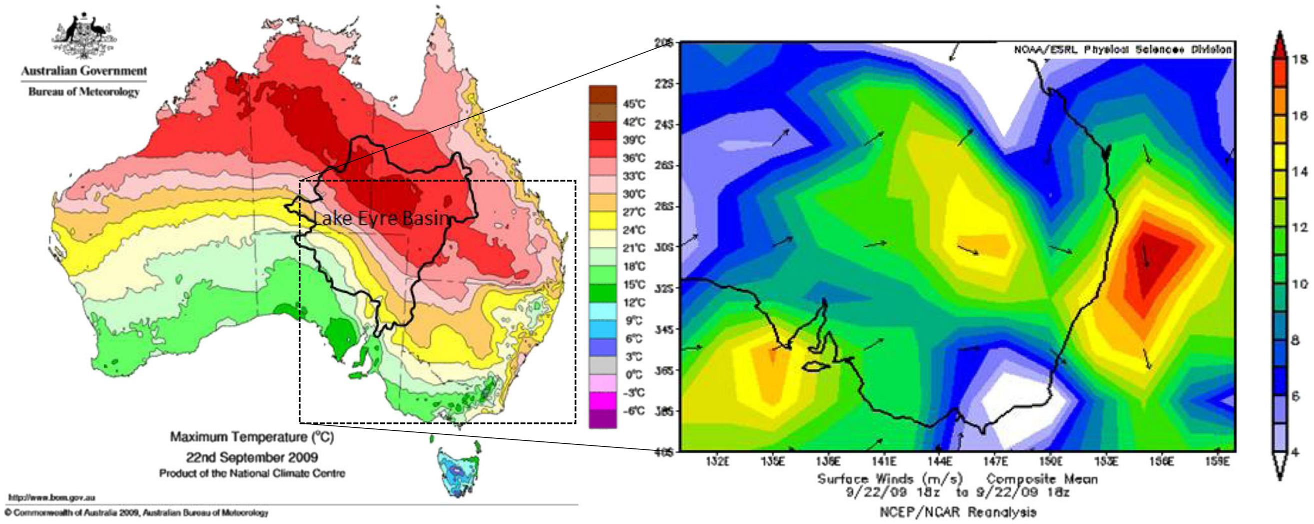

Fig. 2 Mean sea level pressure charts associated with the cold front development in Eastern Australia on 22–24 September 2009

the elemental composition in PM_{10} for source identification.

This study investigates the PM_{10} concentrations, as well as their dynamics during the dust storm at 22 locations across NSW. It also compares the mass size distributions on the day of the dust storm against what was considered a normal day after the dust storm.

Materials and methods

PM_{10} monitoring data was recorded at 22 monitoring stations across NSW before, during, and after the event. This data was obtained from the NSW Environment Protection Authority as an hourly average. PM_{10} samples were also collected near the central business district (CBD) of Sydney, NSW, during the dust storm event (23 September 2009) and 1 week after the event (29 September 2009) using a none-stage cascade impactor (Environmental Tisc, USA). The cascade impactor was placed on the second floor (terrace) of a University of Technology, Sydney (UTS), building in Ultimo (latitude 33.897 and longitude 151.200). The impactor was 8 m above ground level. The building was located 500 m from the CBD and 50 m away from a busy traffic road (>30,000 vehicles per day). The monitoring site represents a typical urban environment which is dominated by vehicular activities.

The dust samples were collected on the filters and were placed in desiccators for 24 h at laboratory temperature (25 °C) to eliminate any remnant moisture on the filters. A gravimetric method (five-digit microbalance, Mettler, Toledo) was used for mass calculation in each fraction. Air flow rates (30 m^3/h for 4 h on the dust storm day and for 24 h a day a week after the event) in the impactor was calculated in the field using a manometer which sensed the pressure drop across the nine stages of the impactor. Quantification of the dust particle fractions collected in the cascade impactor were based on the theoretical impaction curve diagrams provided by the manufacturer (Aryal et al. 2013).

Meteorological data such as temperature, wind speed and direction, and humidity was collected from automatic weather stations across NSW by the Bureau of Meteorology, Australia.

The elemental ratio of PM_{10} collected at the UTS site was studied by applying scanning electron microscopy (environmental scanning electron microscope) equipped with electron diffraction X-ray (Siemens D5000 X-ray Diffractometer) (Aryal et al. 2012). Figure 1b shows the 22 monitoring stations for PM_{10} across NSW.

Statistical analysis

A cumulative sum (CUSUM) method (Kamruzzaman et al. 2011) was implemented to examine evidence of relative changes under the mean. The CUSUM at time n was calculated as:

$$C_t = \sum_{i=1}^{n} \left(x_i - \overline{x}\right)$$

where x_i represents a sample size, and x is the mean of the sample of length n. C_t will have a negative slope if consecutive values tend to lie below the mean, and C_t will have a positive slope if consecutive values tend to lie above the mean.

Results and discussion

Early on 23 September 2009, Sydney was experiencing warm and humid conditions. Northerly winds (bearing of 360°) moving at 8.7 m/s kept the air temperature at 19 °C and the relative humidity was high at >75 % as a result of thunderstorm activity the previous afternoon. The PM_{10} concentration was below 50 μg/m^3 which is the Australian ambient air quality standard over 24 h. As the morning progressed, the PM_{10} concentration slowly increased until it was in excess of 10,000 μg/m^3 at more than 13 locations in the Sydney area within a couple of hours. This corresponded with an increase in the wind speed to 10–12 m/s. Figure 3 shows the measured PM_{10} before, during, and after the dust storm at various locations across NSW (see Appendix 1 for PM_{10} data). This shows that before the event, the PM_{10} value was lower than the Australian guideline value of 50 μg/m^3 in almost all areas except for a few cases across NSW. The wind increased to 10–14 m/s and shifted to a northwesterly direction (bearing of 309.6°) ahead of an approaching cold front. The highest PM_{10} value recorded in Sydney was 11,800 μg/m^3 at Randwick at 7 a.m. Across NSW, the highest value was 15,388 μg/m^3 recorded at Bathurst, which is a regional center located 200 km west of Sydney. From Fig. 1, Bathurst is located in the middle of the dust storm path corridor proposed by Bowler (1976). It has been reported that this storm resulted in the loss of 2.54 million tons of soil off the coast and that the total economic cost was between AUD $418–438 million (Tozer and Leys 2013). This estimated economic loss does not include a further AUD $8.8 million for

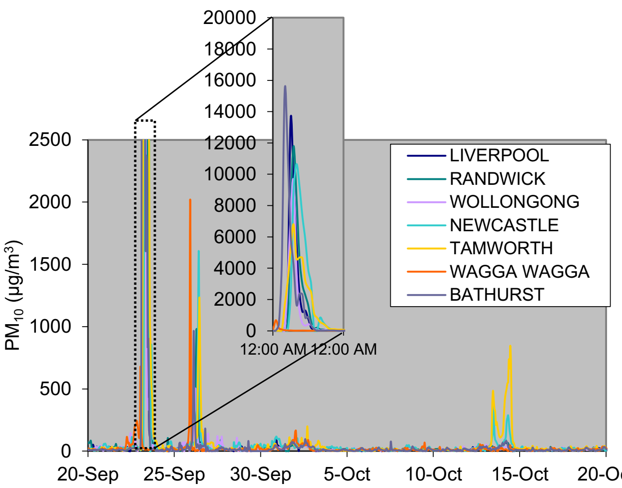

Fig. 3 PM_{10} before, during, and after the 2009 dust storm across NSW, Australia

nutrient loss from agricultural soil, because it was assumed that this would not be replaced by farmers.

Figure 4 shows the PM_{10} dynamics across NSW during the dust storm period. The contour diagrams show that the atmospheric concentrations of PM_{10} before the event (Fig. 4a) were at acceptable levels. Soon after this, the sky was masked with red particles along the south corridor at the beginning and then to the north–south corridor of NSW (Fig. 4b). These diagrams show that the concentrations started increasing on the southern edge of the study area. This was due to strengthening northerly winds transporting the dust from the country's interior. The plume then started to migrate northward as southerly winds behind a cold front started to bring in clearer maritime air from the south. The cold front moved through Wagga Wagga at approximately 2 p.m. on the 22 September. Then, almost 24 h later, the front moved through Sydney airport at around 1.30 p.m. on 23 September. The front continued to move northward to Bathurst by 3 p.m. and to Williamtown (near Newcastle) by 11 p.m.

Once the northerly winds had increased, it was only a few hours before the particle concentrations suddenly jumped to more than 10,000 μg/m^3. The maximum PM_{10} concentration in Sydney was in the range 10,000–13,000 μg/m^3. The other two major east coast cities Wollongong and Newcastle, which are both near Sydney, experienced levels around 10,000 μg/m^3. It was believed that local wind circulation in Sydney might have affected dispersion of particles across a 100-km belt (Fig. 4c, d). Almost 24 h later, the event had passed through Sydney and atmospheric PM_{10} returned back to normal levels (Fig. 4e). Appendix 2 shows the PM_{10} concentrations across NSW at 3-h intervals, before, during, and after the dust storm.

A large variation in PM_{10} concentration along the storm path showed that wind direction played an important role in PM_{10} transport. Figure 2 illustrates the synoptic situation which transported the dust toward the east coast on the day of the event. Up until approximately the midpoint between the dust source and the east coast cities, the dust storm passed as a single plume. However, as it reached the Blue Mountains range, the plume dissipated toward the north east (Queensland) and south east (Canberra region) as well continuing straight ahead to the city of Sydney. This is due to the stalling of the cold front on the higher topography (see Fig. 2).

Figure 5 shows the topography of the Bathurst and Sydney areas and the mountain range (Blue Mountains) that lies between them. The Sydney region also called Sydney Basin is bounded in the west by the Great Dividing Range, called Blue Mountains, which runs parallel to the eastern coast of Australia (Cohen et al. 2011). The Blue Mountains range is

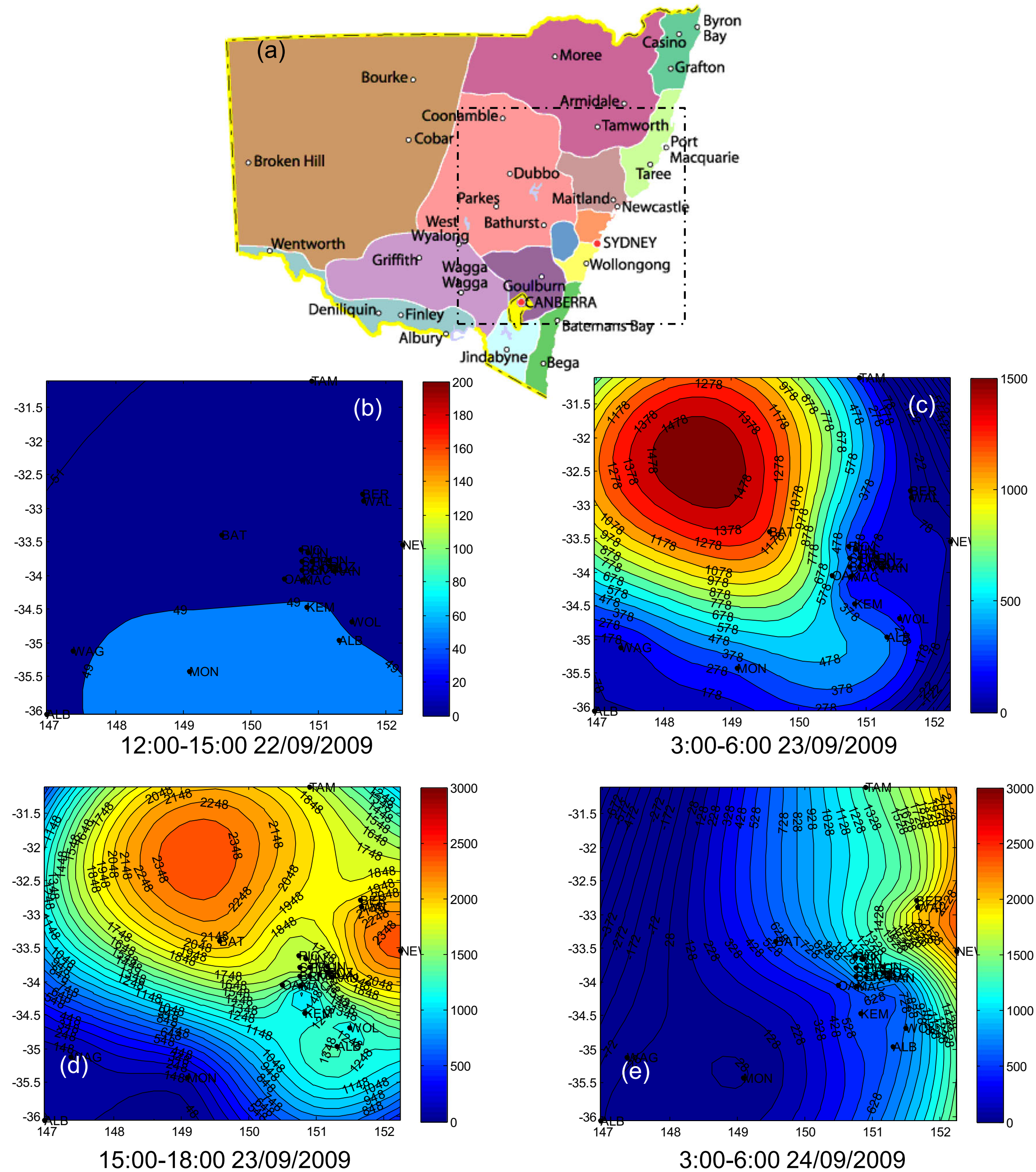

Fig. 4 PM_{10} monitoring sites (*dotted line*) in NSW (**a**) and PM_{10} concentration before (**b**), during (**c**, **d**), and after (**e**) the dust storm across NSW

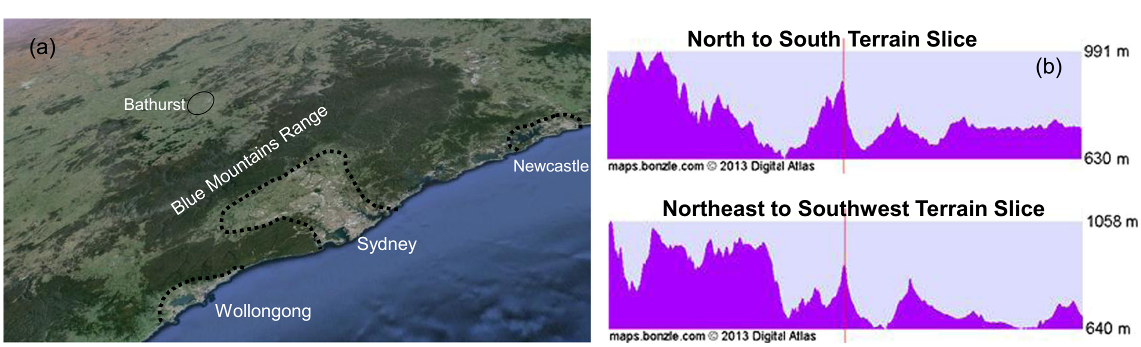

Fig. 5 **a** Topography of three east coast cities, Sydney, Wollongong, and Newcastle, in NSW and **b** topographic profile in north–south, and NE/SW diagonal slices, centered around Blue Mountains

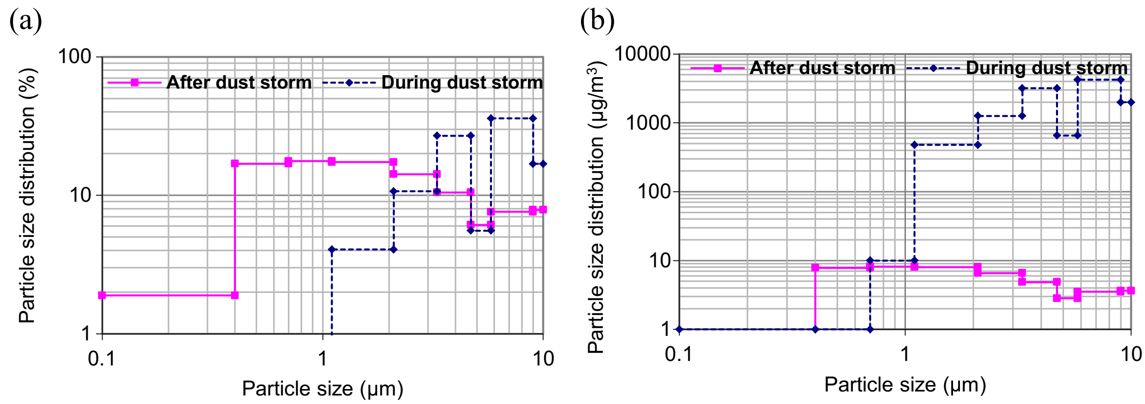

Fig. 6 Particle size distributions during and after the dust storm: particle size distribution **a** with respect to percentages and **b** with respect to concentrations (μg/m^3)

elevated from 600 to 1,030 m. There was a strong fall in PM_{10} concentration from Bathurst (~15,300 μg/m^3) to Sydney (11,800 μg/m^3). This sharp decrease in PM_{10} concentration indicates that the Blue Mountains range played an important role in reducing the dust storm's concentration as it reached the Sydney region. Higher particle density and a steeply sloped mountain range appears to have helped to barricade the dust storm and reduce the PM_{10} concentration by almost 2,000 μg/m^3 (Li et al. 2010). This assumption is supported by further reductions in the PM_{10} concentration in Wollongong (9,600 μg/m^3) (60 km of Sydney) which is also surrounded by a small mountain range.

The Sydney basin is the largest city in Australia with 4.5 million people inhabit the basin with nearly 3 million motor vehicles, and this basin is a natural trap for fine particles produced locally (Cohen et al. 2011). Air pollution is always of great concern in the city due to human-health-related issues caused by topography. Figure 6 shows the particle size distribution of PM_{10} by (a) volume percentage and (b) concentration on normal day (after the dust storm) collected at UTS building. The PM_{10} fraction (graph) suggested that a bimodal distribution (0.1–4.7 and 4.7–10 μm) existed on a normal day (after the dust storm). The finer particle size mode corresponds to the accumulation phase, and the coarser particle size mode corresponds to the mechanical erosion and resuspension of dust particles (Allen et al. 2001; Kulshrestha et al. 2009). Past studies show that most of the aerosol in urban environment is from vehicular emission and exhibit bimodal distribution (Chan et al. 2000; Karanasiou et al. 2007; Lu 2002; Santamaria et al. 1990; Spurny 1996). During the event, particle size fractions appear to display a multimodal distribution (0.1–1.1, 1.1–4.7, and 4.7–10 μm). The multimodal peaks in Fig. 6 suggest that dust from other sources also intruded into the urban aerosol. The thousand-fold increase in finer particles (6–10 μm) in the atmosphere suggests that the particles not only came from external sources but also that they travelled hundreds to thousands of kilometers before reaching Sydney (Knight et al. 1995). Jayaratne et al. (2011) also conducted study on aerosol during the event and on-normal days in Brisbane, almost 1,000 km north of the Sydney sampling station. They observed most of the

Fig. 7 Relative change in particle size distributions for **a** a normal day (after the dust storm) and **b** during the dust storm

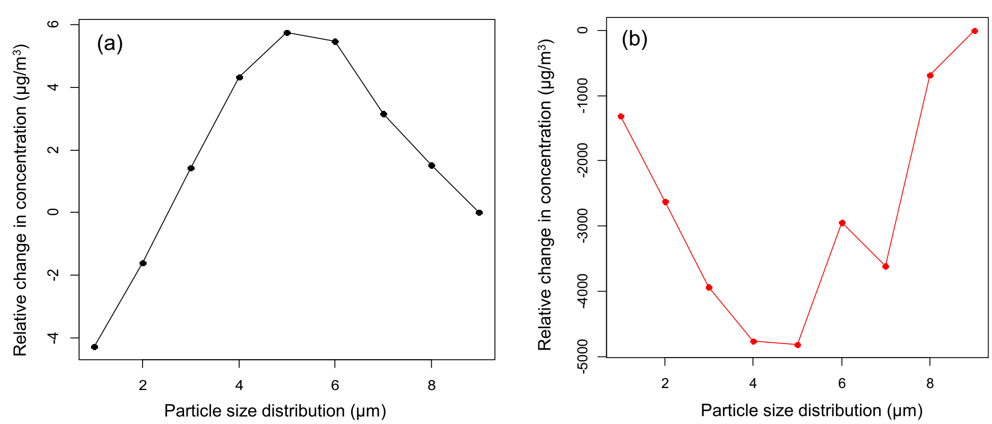

mass in the size range below 10 μm lay between 2.5 and 10 μm, similar to our results.

Figure 7 shows the relative change in particle size after (a) and during (b) the dust storm. This shows significant differences in the relative change in particle size distributions. During a normal day (a), the particle sizes follow a normal distribution whereas during the dust storm, the distribution is not normal and instead displays a multimodal distribution. This results in significant changes in the mass fraction ratio during the dust storm.

The Al/Si ratio is considered a good indicator to distinguish between desert- and anthropogenic-dominated samples with high values in the former group and lower in the latter (Blanco et al. 2003). According to Guerzoni et al. (1997), Al/Si ratios higher than 0.3 are generally indicative of the desert origin of the particles. The PM_{10} Al/Si ratio observed in sample collected in UTS building during the dust storm was 0.39. The higher ratio during the storm indicates that particles originated from desert origins (Blanco et al. 2003; Guerzoni et al. 1997). This high Al/Si ratio of 0.39 is very similar to the values reported by Cohen et al. (2011) in their long-term study (1998–2009) of fine particles in dust storms in the Sydney Basin (median of 0.27, average of 0.30, and maximum of 0.35). The value of 0.14 (for fraction 6–10 μm) is found in the week after the event. This low Al/Si ratio after the storm represents typical urban atmospheric conditions. Marcazzan et al. (2001) recorded 0.35 in PM_{10} in Milan, Italy. Limbeck et al. (2009) observed this ratio 0.17–0.28 in Vienna, Austria. Cohen et al. (2004) calculated Al/Si elemental ratio 0.30 in Hong Kong. Further, our organic carbon analysis showed that the total organic carbon content in the dust storm was 10.6 % (Aryal et al. 2012) which was up to sixfold higher than in urban aerosol organic carbon reported earlier (Didyk et al. 2000; Offenberg and Baker 2000; Viidanoja et al. 2002).

Conclusion

PM_{10} particle size distributions and elemental ratio data were collected from 22 locations across NSW during and after a significant dust storm event in Sydney on 23 September 2009. PM_{10} concentrations were less than 50 $\mu g/m^3$ before the dust storm arrived. The concentration quickly jumped to more than 10,000 $\mu g/m^3$ within a couple of hours of the storm's arrival and then dropped to more normal levels (<50 $\mu g/m^3$). The PM_{10} concentration distribution across NSW showed localized influences on the dust storm. The PM_{10} distribution measured by the cascade impactor showed a bimodal distribution (0.1–4.7 and 4.7–10 μm) on normal days whereas during the dust storm, a multimodal PM_{10} distribution (0.1–1.1, 1.1–4.7, and 4.7–10 μm) was evident. The bimodal distribution showed largely urban sources for PM_{10} whereas the multimodal distribution showed other sources of particulate matter. In particular, approximately 60 % of the dust particles were less than 10 μm and this indicated a long-range transport of dust. The Al/Si ratio during the storm reached 0.39 and then dropped to 0.14 after a week. The high Al/Si ratios (>0.3) indicate that the dust particles originated from inner desert areas of Australia.

Appendix 1

	Liverpool	Prospect	Macarthur	Bringelly	Chullora	Randwick	Rozelle	Richmond	Lindfield	St Marys	Vineyard	Albion Park
Latitude	33.93	33.79	34.07	33.90	33.89	33.93	33.87	33.62	33.78	33.80	33.66	34.58
Longitude	150.91	150.91	150.78	150.76	151.05	151.24	151.16	150.75	151.15	150.77	150.85	150.79
22/09 1:00	17.2	15.2	16.5	17.4	17.7	17.9	18.9	19.1	16.9	13.7	17	22.3
2:00	15.9	14.5	17.6	24.3	18.2	17.2	19.8	8.3	17.7	7.4	15.4	18.1
3:00	14.6	13.9	15	25	14	19.5	17	11.3	12.8	6.5	12.9	20.6
4:00	14.7	14.4	14.1	20.4	14.7	22.1	18.8	18.9	14	13.6	14.4	20.8
5:00	14.9	11.1	18	10.1	18.3	24.5	18.9	14.2	10.6	16.6	12.6	17.8
6:00	14.2	9.1	18.5	7.6	48.1	5.5	6.4	8.9	9.9	7.8	9.1	17.6
7:00	33.3	12.1	22.1	22.3	91.3	12.8	8.2	13.3	9.6	13.8	9	19
8:00	17.5	14.5	21.1	29	35.2	11.6	11.5	15	13	23.4	14.6	20.7
9:00		25.6	22.1	27.8	22	21.2	20.4	19.9	17.9	15.8	14.2	37.8
10:00		28.8	51	42.9	43.9	31	28.6	22.4	21.7	18.6	16.9	305.7
11:00		27.8	50.9	55	35.9	30.8	30.7	41.2	22.2	30.9	30.5	342.1
12:00	51.7	49.5	38.4	62.2	61.4	36.2	29.3	80.4	33.2	44.5	46.9	186.3
13:00	60.5	46.4	41.7	63.7	97	39.8	43.1	38.4	36	46.4	41.7	75.7
14:00	40.7	40.5	59.7	44.3	69.1	45.3	39.8	35.9	44.5	39	44.5	59.4
15:00	48.1	44.7	69.7	53	78.3	43.5	50.3	39	47.6	45.5	42.3	69.5
16:00	48.7	38.4	66.3	53.4	54.1	41.8	42	34.7	40	43.8	35	93
17:00	50.7	40.9	61.9	62.5	52	42.1	38.7	27.8	30.6	48.1	32.4	119.6

18:00	40.2	38.2	56.7	48.6	38	36.2	35.5	32	26.7	39	36.9	121.5
19:00	46	50	28.9	44.3	62.4	48.6	53	45.3	34.7	43.4	44.8	16.1
20:00	4.9	4.7	5.7	4.5	7	12.2	23.4	10	19.3	0.7	11	10.7
21:00	11.2	12.3	6.4	15.2	15.7	13.3	15.6	14	14.7	12.2	10.8	11.8
22:00	6	8.6	9.9	11	11.2	11.5	8.8	17.4	15.8	8.3	14.4	9.6
23:00	13.4	11.1	13.8	15.6	11.3	12.6	8.8	13.6	9.7	14.3	16.8	13.7
23/09 0:00	13.4	17.5	15.1	16.1	16.2	14.5	13.4	20.6	14.8	15.7	17.5	17.6
1:00	10.8	16.9	11.7	12.4	11.9	6	7.4	10.6	12.2	8.3	7.7	12.1
2:00	16.3	14.8	15.2	16.3	17.3	16.9	15.7	10.6	14.7	10.7	12.4	21.1
3:00	14.3	27.1	13.1	21.9	46.6	39.3	73.6	20	71.3	10.7	28.3	15.4
4:00	47.4	98.6	38.8	36.9	92	79.4	96.2	331.7	77.3	77.1	180	340.1
5:00	2,559.9	2,151.5	1,983.4	5,238.9	1,155.3	518.2	627.4	5,039	690.6	4,758.8	4,216.2	5,470.7
6:00	13,516	11,682.3	10,282.1	15,366.1	10,220	7,714.1	7,333	11,160	7,570.7	13,888	11,174.4	10,995.3
7:00	9,650.5	10,871.2	8,127.6	9,477.3	9,758.2	11,799	10,083	8,422.1	9,538.8	10,009.2	9,656.6	11,376.8
8:00	5,574.4	5,193.4	3,045.3	4,888.2	5,459	8,530.1	7,283.2	3,575.8	6,989.5	3,607.9	3,569.1	1,849.8
9:00	2,446.6	3,518.3	1,643.8	1,703.7	3,210.1	4,699.1	4,147.2	3,624.8	4,534.2	2,472.7	4,366.5	894.8
10:00	1,223.3	2,024.8	724.9	1,026.6	1,776.8	2,964	2,824	2,499.1	3,001.3	1,710.6	2,697.8	439.2
11:00	1,297.4	2,163.9	396.1	1,052.9	1,706.2	2,277.6	2,415.3	2,104.5	2,632.6	1,701.8	2,485.7	297.3
12:00	773	1,535.2	231.1	665.6	1,079.8	1,621.7	1,444.4	1,161.7	1,739.2	833.9	1,117.3	313.1
13:00	195.2	358	416	170.3	284	566.7	445.6	699.2	587.5	237.1	562	134.2
14:00	113.5	213.4	213.5	226.5	123.1	183.3	219.3	283.1	379.7	159.8	319.8	105.4
15:00	103.7	99.7	64.7	71.6	86.6	195.8	105.3	124	144.5	69.5	119.5	58.7
16:00	68.1	53.6	50.3	76.7	42.4	98	51.7	38	66	42.5	49.2	22.3
17:00	77.5	21	40.1	93.6	109	80.8	35.4	39	42.2	1	36.6	66.1
18:00	32.9	50.2	34.7	61.1	56.3	34.5	70.9	33.8	23.1	47.9	23.8	51.1
19:00	27.4	67.5	43.4	41.8	22.5	28.5	44.6	22.1	45.8	43.6	26.5	44.2
20:00	41.8	2.7	34.6	35.9	27.8	57.9	33.6	15.3	21.1	51.6	22.5	57
21:00	43.4	58.1	40.9	41.9	34.4	44.8	51.5	18.9	35.3	23.3	22.1	44.2
22:00	41.9	43.3	23.9	41.2	36.2	43.1	48.2	31.2	43	35	41.7	12.1
23:00	20.7	40.8	19.6	24.9	22.3	31.9	28	12.9	29.4	17.8	17.9	2.1
24/09 0:00	18.7	20.1	15.2	21.5	15.6	24.3	23.8	18	20.6	47.7	19.1	7.9
1:00	16.1	31.6	2.7	16.7	18.9	15.3	19.9	14.5	21.2		25.7	7.5
2:00		3.3	13.5	4.9		11.6			20	13.5	7.8	3
3:00	15.4	2.1	6	13.2	10.3	2.6	6.2		2.7			13.4
4:00	5.6	24.5	4.3	9.9	5.4	5.6	12.7	8.6	15.3	18.1		
5:00		14.8	9.7	5	3.1	2.9	8.8	16.5	24	25.5	16.4	11.3
6:00	13.2	18.3	18.1	14.3	17.8	3.8	11	2.2	10	25.3	19.1	10.5
7:00	21.7	40.9	17.8	21.3	26.1	26.8	22.6	71.5	23.4	40.2	30.6	20.8
8:00	13.1	7	8.3	18.6	20.6	23.2	22.7		18.9		12.9	6.3
9:00	10.8	7.9	11.1	1.8	13.7	10.6	9.1	18	6.4	12.8		12
10:00	2.9	11.6		5.2	14.5		15.6	18.3	14.7	12.8	6.9	6.3
11:00		12.3			10.6	6.2			6.8	8.9	9.2	
12:00	6.7		11	11.5	8.5	21.6	10.8	14.9		2		
13:00	18.7	23.9	11.1	29.7	16.7		15.3	32.3	30.8	43.5	25.9	47.5
14:00	29.3	33.5	11.5		33	24.4	31.9		20.8		19.8	40.3
15:00			13.6		9.1	106	22.8		6.7	23.6	11.1	29.5
16:00			18.7	47.5	29.2	33.9	15.7	11.7	14.2	19.5	27.1	27.3
17:00		4.2	13.1	37.9	26.9		39.5	13.6	28.8	18.4	25.6	24.5
18:00	58	10.2	11.9	30.4	25	27.1	15.3	13	23.3	10.8	3.8	23.4
19:00	39.5	12.2	8.6	26.1	23.6	12	26	14.1	19.8	3.7	4.9	18.9
20:00	30.9	10.2	10.6	20	6.9	4.9	7.7	10.2	11.2	11.1	5.3	16.7
21:00	24.4	8.4	7.1	18.8	14.2	12.1	11	10.7	16.5	7.6	15.7	16.8
22:00	21.1	10.7	7.1	17.7	12.2	12.5	19.1	11.7	13.3	17.2	21.7	14.5
23:00	23	11	6.7	20.7	25.9	13.4	24.2	12	15.5	31.4	15.3	14

	Wollongong	Kembla Grange	Wallsend	Newcastle	Beresfield	Tamworth	Albury	Wagga Wagga	Bathurst	Monash, ACT
Latitude	34.42	34.48	32.90	32.93	32.80	31.11	36.05	35.10	33.40	35.43
Longitude	150.89	150.82	151.67	151.76	151.66	150.91	146.97	147.36	149.57	149.10
22/09 1:00		18.3	17.7	28.5	20.3	3.6	14.4	9.1	8.7	11.5
2:00		18.3	19.7	29.2	21.9	6.2	12.8	8.5	4.5	12.0
3:00	30.4	19.5	8.7	21.7	20.5	6.4	25.7	14.4	4.5	4.5
4:00	40.5	22.2	8.2	17.4	22.9	5.8	36.7	28.5	4.5	14.0
5:00	25.3	18.8	5.9	24.1	19.3	9.9	65.2	52.7	6.9	9.0

6:00	16.3	16.9	15.2	25.3	17.9	9.2	55.1	114	9.3	5.5
7:00	17	18.4	31.4	26	19.4	16.4	19.2	89.7	13.7	3.5
8:00	21.4	28.1	20.1	20.3	20.7	13.5	23.7	61.1	15.2	29.5
9:00	39.7	93.5	22.1	21.4	16.9	17.6	17.6	67.3	18.7	148.5
10:00	80.7	266.2	36.4	36.1	29.9	20.1	10.3	24	19.4	209.5
11:00	144.3	289.9	46.8	39.1	37.4	34.7	4.5	39.6	31.1	166.0
12:00	132.4	175.4	54.4	48.2	57.7	31.5	6.2	52.1	19.9	132.5
13:00	63.1	90	110.2	113.8	44.7	20.4	5	56.4	22	100.5
14:00	52.4	76.5	47.4	43.9	17.5	24.4	6	53.3	23.1	262.5
15:00	55.3	69.9	29.3	28.3	10.5	19	7.6	81.9	23.6	630.5
16:00	67.2	128.6	25.9	23.6	15.6	19.8	6.7	138.9	22.9	851.0
17:00	74.6	125.1	27.5	25.1	19.4	19.3	5.8	196.5	26.8	681.0
18:00	86.1	73.7	25.9	18.7	17.1	21.3	13	213.1	25.8	586.5
19:00	13.2	13.6	23.6	22.2	19	17.9	10.3	210.1	4.4	497.0
20:00	11.1	11.8	15.8	17.1	17.1	15.4	12.3	243.2	10.8	418.5
21:00		8.4	16.7	22.4	22.5	10.6	8.8	210.4	11.5	123.5
22:00	10	34.5	25.1	32.2	28.9	11.8	5.5	154.3	18.1	46.5
23:00	16.7	17.1	15.2	17.8	17.8	14.2	6.8	105.7	17.1	33.5
23/09 0:00	21	20.7	11.2	14.2	12.2	26.2	5.6	105.4	18.6	35.5
1:00	16	14.7	6.6	6.6	7.6	18	21.1	679.7	28.7	33.5
2:00	20.9	24.2	11.8	11.8	6.8	10.9	50	178.6	424.6	32.5
3:00	19.6	20	30.9	18.1	22.5	41.1	51.3	87.4	4,268.2	36.5
4:00	20.5	141.4	63.2	59	27.6	1,631.4	53	40.8	15,388.2	
5:00	3,193.9	4,503.9	34.4	26.3	25.3	3,128.5	45	24	11,512.1	1,475.0
6:00	7,406.4	8,408.1	2,590.4	2,253	3,987.7	5,216.9	53	23.9	6,186.6	710.0
7:00	9,576.9	9,481.8	7,962.1	8,967.3	8,362.4	6,804.6	49.3	13.7	4,238.5	179.5
8:00	3,801.9	1,939.7	8,997.4	10,651.2	9,209.8	4,576.8	18.2	11.4	1,667.9	75.0
9:00	1,297.1	1,085.8	7,620.3	9,282.1	7,023.6	4,685.5	15	14.2	2,371.5	15.0
10:00	482.2	486.5	6,255.6	7,322.4	6,437.4	4,650.2	16.5	18	2,314.5	
11:00	333.8	492.1	4,875.9	5,811.7	4,472.6	3,173.8	14.9	14.3	837.4	1.5
12:00	420.8	870.3	2,985.8	3,894.3		2,757.6	10.8	8.6	905.3	
13:00	356.3	219.7	2,490.2	2,940.1		2,451.7	13.7	9.1	345.4	0.5
14:00	130.9	123.1	1,759		1,764.4	1,090.3	12.6	13.2	115.7	2.5
15:00	98.6	119.6	976.8		980.7	840.1	10.1	11.1	13.4	10.0
16:00	30	55.2		838	671.3	566.8	13.9	15.8	15.2	7.5
17:00	49.4	46		564.6	401.1	461	9.5	13.1	12.1	3.0
18:00	48.9	46	303.2	331	266.8	321	8.3	17.1	19	9.5
19:00	21.8	12.4	149.7	178.9	115.5	144.3	7.5	13.2	22.1	5.5
20:00	28.2	19.9	72.6	87.3	65.7	104.3	9.1	11.9	23.1	7.5
21:00	84.7	29.1	44.3	54.5	42.1	104.3	4.9	9.2	20.7	2.0
22:00	19.6	14.4	31.4	37.9	34.1	76.7	4.3	10.8	5.3	4.0
23:00	8.2	7.7	25.7	32.1	30.9	80.2	4.6	7.9	0.1	2.5
24/09 0:00	22	15	19.1	22.1	22.7	58.5	4.2	6.1	9.4	4.0
1:00	13.8	13.6	13.4	19.1	26	42.7	5	3.4		0.5
2:00	10.3	1.2	17.1	18.6	28.9	32.8	4.2	5.3	3.2	2.0
3:00		8	16.7	23.3	26.8	21.4	5.8	5.9		0.5
4:00		0.7	18.6	23.5	27.3	20.9	5.6	5.6	6.7	
5:00	15.5	17	18.1	21.7	23.8	16.1	6.6	7.2	9.4	3.5
6:00	17	10.3	16.2	21.6	22	10.4	5.7	9.1	0.1	0.5
7:00	16.3	16.5	19.3	21.4	25.4	19.3	9.1	7.8	13.5	
8:00	8.7	11.7	19.1	23.2	23.7	48.1	10.6	9		
9:00	13.2	18.8	17.4	23	20.3		12.7	13.5		3.0

10:00	13.3	16.8	23.5	22.8	23.3		14	8.1		
11:00		2.9	17.3	22.9	24	20	10.9	4.7		7.0
12:00	15.2	21.6	17.7	18.1	17.3	9.5	13.7	8	4.4	2.5
13:00	9.5		40.9	22.9	22.9		9.6	11.3	27.2	
14:00	23.2		32.5	38.7	33.9		9.1	4.9	11.2	
15:00	7.6	14.7	38	42.1	31.5	39.8	12.8		16.3	6.5
16:00	13.7	26.6	34.6	38.4	28.2	32.7	12.1	10.1	15.3	
17:00	17.7	23.4	26	52.1	25.8	35.2	13.5	12.2	1.8	6.0
18:00		11	20.4	52.4	26.3	44.1	13.8	14.6	0.4	2.5
19:00	11	10.3	22.7	79.6	27.2	21	16.8	18.1	29.9	9.0
20:00	30.5	10.6	29.8	67.1	35.1	31.6	14	22.8	38	0.0
21:00	16.5	8.6	25	22.1	32	22.7	16.8	31.1	27.8	6.0
22:00	6.2	7.8	19.2	19.7	29.8	26.5	17.8	24.2	1.5	7.5
23:00	8.9	8.7	12.4	6.3	19.9	25.6	6	23.9	4.8	8.0

Appendix 2. PM_{10} concentration before, during, and after the dust storm across NSW every 3 h

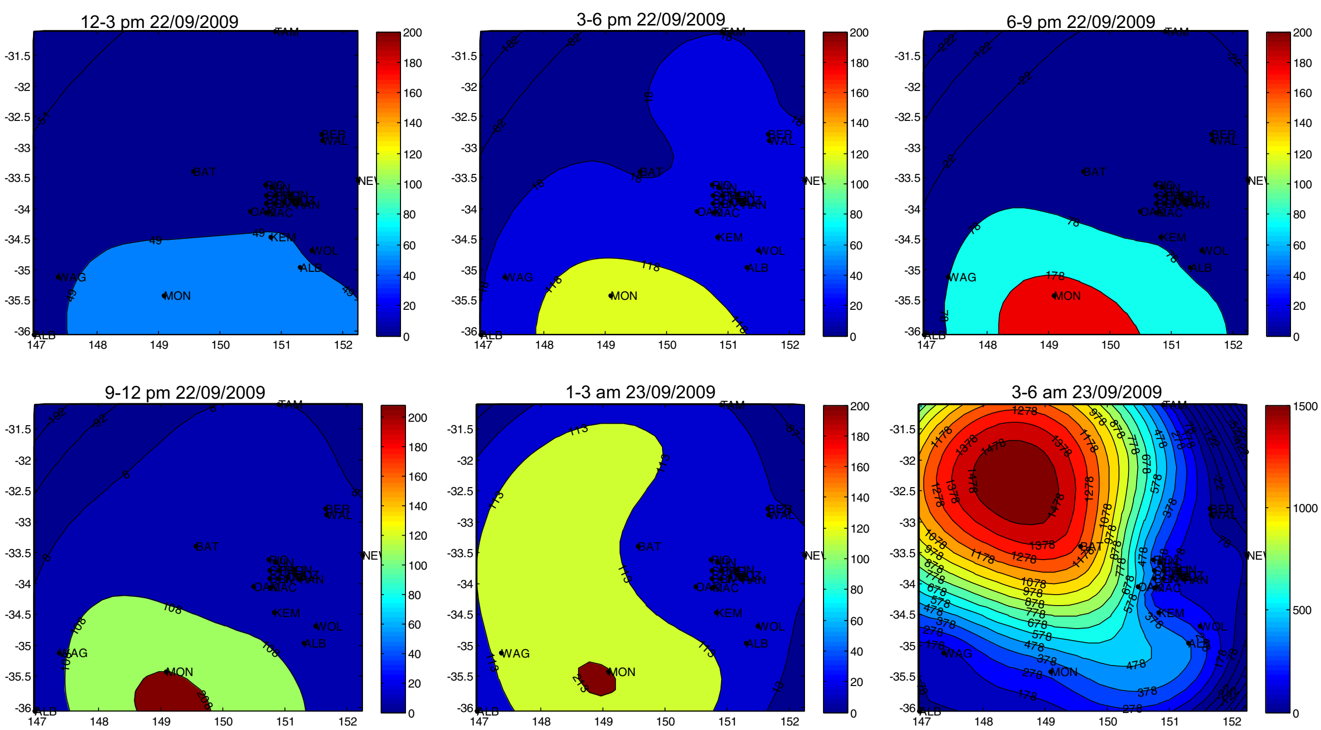

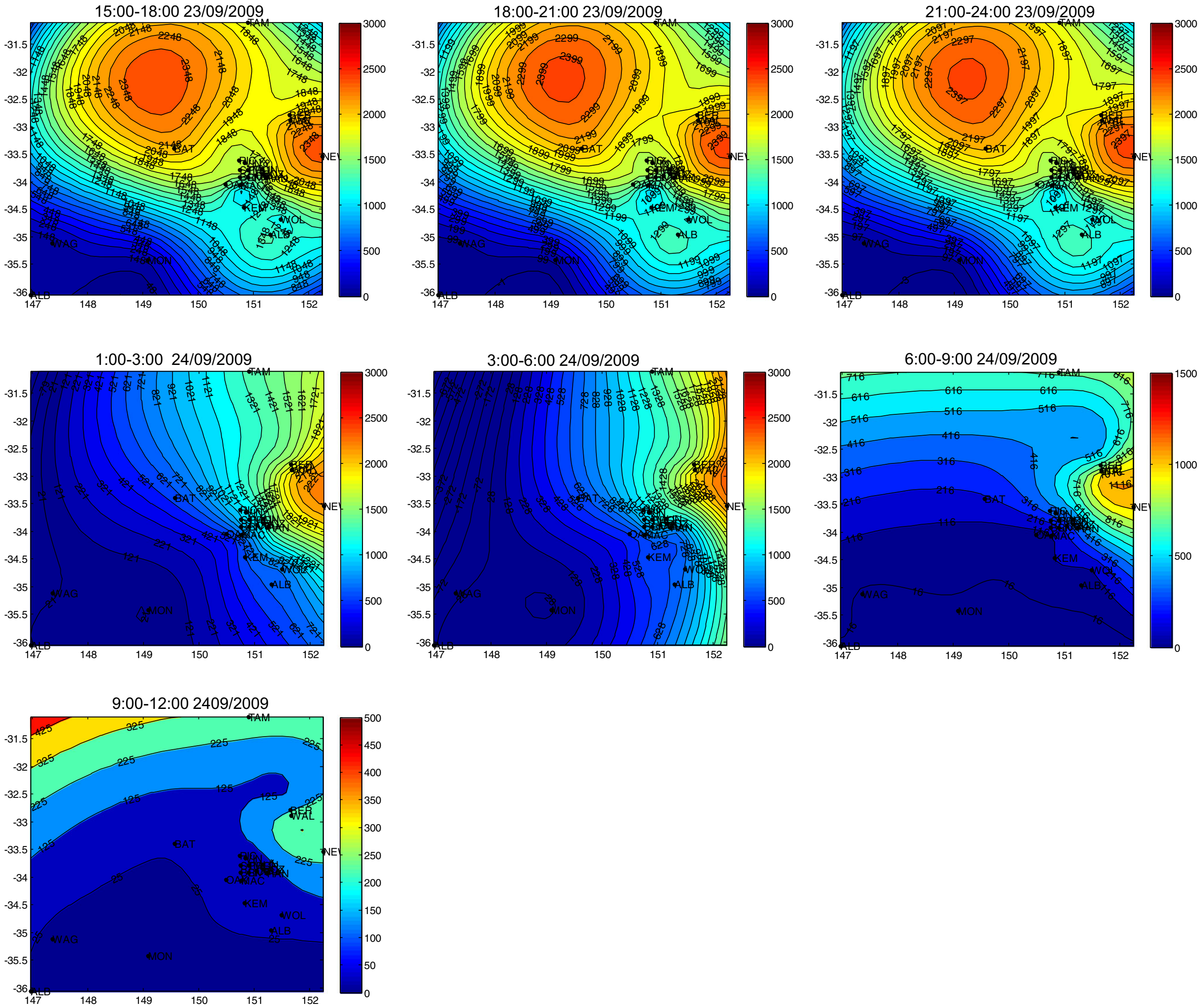

References

Allen AG, Nemitz E, Shi JP, Harrison RM, Greenwood JC (2001) Size distributions of trace metals in atmospheric aerosols in the United Kingdom. Atmos Environ 35:4581–4591. doi:10.1016/S1352-2310(01)00190-X

Aryal RK et al (2008) Seasonal PM10 dynamics in Kathmandu Valley. Atmos Environ 42:8623–8633

Aryal R, Kandel D, Acharya D, Chong MN, Beecham S (2012) Unusual Sydney dust storm and its mineralogical and organic characteristics. Environ Chem 9:537–546. doi:10.1071/EN12131

Aryal R, Kim A, Lee B-K, Kamruzzaman M, Beecham S (2013) Characteristics of atmospheric particulate matter and metals in industrial sites in Korea. Environ Pollut 2:10–21. doi:10.5539/ep.v2n4p10

Ayala A, Brauer M, Mauderly JL, Samet JM (2012) Air pollutants and sources associated with health effects. Air Qual Atmos Health 5:151–167

Blanco A, de Tomasi F, Filippo E, Manno D, Perrone MR, Serra R, Tafuro AM, Tepore A (2003) Characterization of African dust over southern Italy. Atmos Chem Phys Discuss 3:2147–2159. doi:10.5194/acpd-3-4633-2003

Bowler JM (1976) Aridity in Australia: age, origins and expression in aeolian landforms and sediments. Earth Science Reviews, 12:279–310

Chan YC, Vowles PD, McTainsh GH, Simpson RW, Cohen DD, Bailey GM, McOrist GD (2000) Characterisation and source identification of PM10 aerosol samples collected with a high volume cascade impactor in Brisbane (Australia). Sci Total Environ 262:5–19. doi:10.1016/S0048-9697(00)00571-4

Cohen DD et al (2004) Multielemental analysis and characterization of fine aerosols at several key ACE-Asia sites. J Geophys Res D-Atmos 109(D19S12):11–18

Cohen DD, Stelcer E, Garton D, Crawford J (2011) Fine particle characterisation, source apportionment and long range dust transport into the Sydney Basin: a long term study between 1998 and 2009. Atmos Pollut Res 2:182–189

Didyk BM, Simoneit BRT, Alvaro Pezoa L, Luis Riveros M, Anselmo Flores A (2000) Urban aerosol particles of Santiago, Chile: organic content and molecular characterization. Atmos Environ 34:1167–1179. doi:10.1016/S1352-2310(99)00403-3

Donaldson K, MacNee W (2001) Potential mechanisms of adverse pulmonary and cardiovascular effects of particulate air pollution (PM10). Int J Hyg Environ Health 203:411–415

Ekström M, McTainsh GH, Chappell A (2004) Australian dust storms: temporal trends and relationships with synoptic pressure distributions (1960–99). Int J Climatol 24:1581–1599

Goldberg MS, Burnett RT, Yale J-F, Valois M-F, Brook JR (2006) Associations between ambient air pollution and daily mortality among persons with diabetes and cardiovascular disease. Environ Res 100:255–267

Guerzoni S, Molinaroli E, Chester R (1997) Saharan dust inputs to the western Mediterranean Sea: depositional patterns, geochemistry and sedimentological implications. Deep-Sea Res II Top Stud Oceanogr 44:631–654. doi:10.1016/S0967-0645(96)00096-3

Jayaratne ER, Johnson GR, McGarry P, Cheung HC, Morawska L (2011) Characteristics of airborne ultrafine and coarse particles during the Australian dust storm of 23 September 2009. Atmos Environ 45: 3996–4001. doi:10.1016/j.atmosenv.2011.04.059

Kamruzzaman M, Beecham S, Metcalfe AV (2011) Non-stationarity in rainfall and temperature in the Murray Darling Basin. Hydrol Process 25:1659–1675. doi:10.1002/hyp.7928

Kan H, Chen B (2003) Air pollution and daily mortality in Shanghai: a time-series study. Arch Environ Health 58:360–367

Karanasiou AA, Sitaras IE, Siskos PA, Eleftheriadis K (2007) Size distribution and sources of trace metals and n-alkanes in the Athens urban aerosol during summer. Atmos Environ 41:2368–2381. doi:10.1016/j.atmosenv.2006.11.006

Kim KW, Kim YJ, Oh SJ (2001) Visibility impairment during Yellow Sand periods in the urban atmosphere of Kwangju, Korea. Atmos Environ 35:5157–5167

Knight AW, McTainsh GH, Simpson RW (1995) Sediment loads in an Australian dust storm: implications for present and past dust processes. CATENA 24:195–213. doi:10.1016/0341-8162(95)00026-O

Kuenzli N et al (2000) Public-health impact of outdoor and traffic-related air pollution: a European assessment. Lancet 356:795–801

Kulshrestha A, Satsangi PG, Masih J, Taneja A (2009) Metal concentration of PM2.5 and PM10 particles and seasonal variations in urban and rural environment of Agra, India. Sci Total Environ 407:6196–6204

Lee BK, Lee CH (2008) Analysis of acidic components, heavy metals and PAHS of particulate in the Changwon-Masan area of Korea. Environ Monit Assess 136:21–33

Leys JF, Heidenreich SK, Strong CL, McTainsh GH, Quigley S (2011) PM10 concentrations and mass transport during "Red Dawn"—Sydney 23 September 2009. Aeolian Res 3:327–342

Li X, Ge L, Dong Y, Chang H-C (2010) Estimating the greatest dust storm in eastern Australia with MODIS satellite images. In: Geoscience and Remote Sensing Symposium (IGARSS), 2010 I.E. International. 2010 IEEE, pp 1039–1042

Lim JM, Lee JH, Moon JH, Chung YS, Kim KH (2010) Airborne PM10 and metals from multifarious sources in an industrial complex area. Atmos Res 96:53–64

Limbeck A, Handler M, Puls C, Zbiral J, Bauer H, Puxbaum H (2009) Impact of mineral components and selected trace metals on ambient PM10 concentrations. Atmos Environ 43:530–538

Lu H-C (2002) The statistical characters of PM10 concentration in Taiwan area. Atmos Environ 36:491–502

Lyamani H, Olmo F, Alados-Arboledas L (2005) Saharan dust outbreak over southeastern Spain as detected by sun photometer. Atmos Environ 39:7276–7284

Marcazzan GM, Vaccaro S, Valli G, Vecchi R (2001) Characterisation of PM10 and PM2.5 particulate matter in the ambient air of Milan (Italy). Atmos Environ 35:4639–4650

McTainsh G, Lynch A, Tews E (1998) Climatic controls upon dust storm occurrence in eastern Australia. J Arid Environ 39:457–466

Mehta S et al (2013) Air pollution and admissions for acute lower respiratory infections in young children of Ho Chi Minh City Air Quality. Atmos Health 6:167–179

Middleton NJ (1984) Dust storms in Australia: frequency, distribution and seasonality. Search 15:46–47

Offenberg JH, Baker JE (2000) Aerosol size distributions of elemental and organic carbon in urban and over-water atmospheres. Atmos Environ 34:1509–1517. doi:10.1016/S1352-2310(99)00412-4

Ostro B, Chestnut L, Vichit-Vadakan N, Laixuthai A (1999) The impact of particulate matter on daily mortality in Bangkok, Thailand. J Air Waste Manag Assoc 49(SPEC. ISS.):100–107

Radhi M, Box MA, Box GP, Mitchell RM, Cohen DD, Stelcer E, Keywood MD (2010a) Optical, physical and chemical characteristics of Australian continental aerosols: Results from a field experiment. Atmos Chem Phys 10:5925–5942

Radhi M, Box MA, Box GP, Mitchell RM, Cohen DD, Stelcer E, Keywood MD (2010b) Size-resolved mass and chemical properties of dust aerosols from Australia's Lake Eyre Basin. Atmos Environ 44:3519–3528

Ragosta M, Caggiano R, D'Emilio M, Sabia S, Trippetta S, Macchiato M (2006) PM10 and heavy metal measurements in an industrial area of southern Italy. Atmos Res 81:304–319

Santamaria J, Fernández M, Mendez J, Bomboi M (1990) Particle size distribution of metals in the atmosphere of Madrid (Spain) Freseniu's. J Anal Chem 337:362–365

Spurny KR (1996) Aerosol air pollution its chemistry and size dependent health effects. J Aerosol Sci 27:S473–S474

Stefanski R, Sivakumar M (2009) Impacts of sand and dust storms on agriculture and potential agricultural applications of a SDSWS. In: IOP Conference Series: Earth and Environmental Science. vol 1. IOP Publishing, p 012016

Strong CL, Parsons K, McTainsh GH, Sheehan A (2011) Dust transporting wind systems in the lower Lake Eyre Basin, Australia: a preliminary study. Aeolian Res 2:205–214. doi:10.1016/j.aeolia.2010.11.001

Tozer PR (2012) The cost of red dawn to the NSW economy. 56th Conference on Australian Agricultural and Resource Economics Society, Fremantle

Tozer P, Leys J (2013) Dust storms—what do they really cost? Rangel J 35:131–142. doi:10.1071/RJ12085

Vanderstraeten P et al (2008) Dust storm originate from Sahara covering Western Europe: a case study. Atmos Environ 42:5489–5493. doi:10.1016/j.atmosenv.2008.02.063

Viidanoja J, Sillanpää M, Laakia J, Kerminen V-M, Hillamo R, Aarnio P, Koskentalo T (2002) Organic and black carbon in PM2.5 and PM10: 1 year of data from an urban site in Helsinki, Finland. Atmos Environ 36:3183–3193. doi:10.1016/S1352-2310(02)00205-4

Wang X, Oenema O, Hoogmoed W, Perdok U, Cai D (2006) Dust storm erosion and its impact on soil carbon and nitrogen losses in northern China. Catena 66:221–227

Washington R, Todd M, Middleton NJ, Goudie AS (2003) Dust-storm source areas determined by the total ozone monitoring spectrometer and surface observations. Ann Assoc Am Geogr 93:297–313

Watanabe M et al (2011) Correlation between Asian dust storms and worsening asthma in Western Japan. Allergol Int 60:267

Xie S, Yu T, Zhang Y, Zeng L, Qi L, Tang X (2005) Characteristics of PM10, SO2, NOx and O3 in ambient air during the dust storm period in Beijing. Sci Total Environ 345:153–164. doi:10.1016/j.scitotenv.2004.10.013